Supporting Information

Selenide-containing Organic Resonance Molecules as Turn-on Fluorescent Probes for Selective Detection of Hypochlorous Acid

He Jiang, Linlin Jia, Yuanyuan Li, Sirui Liu, Runfeng Chen,* Lu Jin, Jibiao Jin, Quli Fan* and Wei Huang*

Key Laboratory for Organic Electronics and Information Displays & Jiangsu Key Laboratory for Biosensors, Institute of Advanced Materials (IAM), Jiangsu National Synergetic Innovation Center for Advanced Materials (SICAM), Nanjing University of Posts & Telecommunications, 9 Wenyuan Road, Nanjing 210023, China.

E-mail: iamrfchen@njupt.edu.cn; iamqlfan@njupt.edu.cn; iamwhuang@njtech.edu.cn

Contents

1. General Experimental Section

Materials: Starting materials, unless otherwise specified, were purchased from commercial suppliers and used without further purification. Manipulations involving air-sensitive reagents were performed in an atmosphere of dry nitrogen. Tetrahydrofuran (THF) were dried and purified by routine procedures.

Instruments: ^{1}H, ^{13}C, ^{31}P and ^{77}Se-nuclear magnetic resonance (NMR) spectra were recorded on a Bruker UltraShield Plus 400 MHz instrument with DMSO-d_6 or $CDCl_3$ as the solvents. ^{1}H and ^{13}C NMR chemical shifts are in ppm relative to tetramethylsilane (TMS) as the internal standard. ^{31}P NMR chemical shifts were calibrated using 85% phosphoric acid as the external standard. The quoted chemical shifts are in *ppm* and the *J* values are expressed in Hz. The splitting patterns have been designed as follows: s (singlet), d (doublet), t (triplet), dd (doublet of doublets), and m (multiplet).

Solubility tests: Solubilities of the N-P=Se resonance molecules in tetrahydrofuran (THF), toluene, dichloromethane (CH_2Cl_2), and trichloromethane ($CHCl_3$) were measured at room temperature. Firstly, the molecule powder (200 mg) was added into the solvent (0.5 mL) equipped with a magnetic stirrer. Secondly, after stirring at room temperature for 24 h, the insoluble residue was filtered, dried and weighted. Finally, from the difference between weights of the initial feeding and the insoluble residue, the weight of the dissolved part can be figured out and the solubility in the solvent was achieved.

2. Previously reported selenium-containing HClO fluorescent probes

In the literature, a wide range of selenium-containing organic fluorescent molecules have been developed for the detection of HClO, as typically illustrated in **Scheme S1**[1-7]. All these molecules were found to change from selenides to selenoxides after the reaction with HClO during the probing processes.

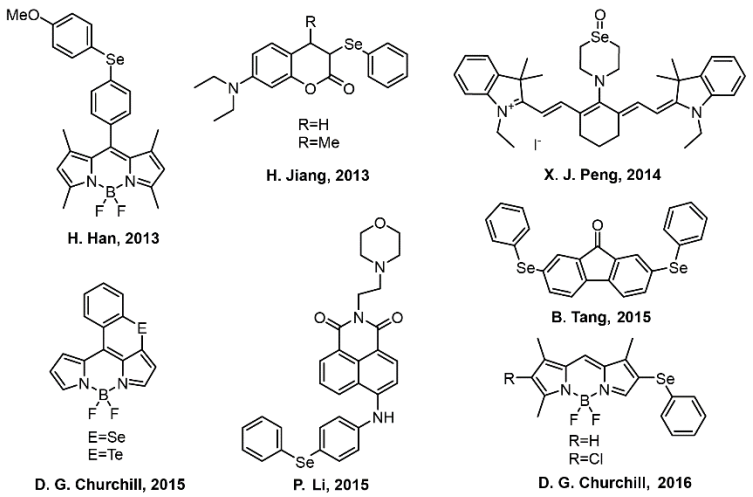

Scheme S1. Selenium-containing fluorescent probes for the detection of HClO.

3. Main Resonance Structures

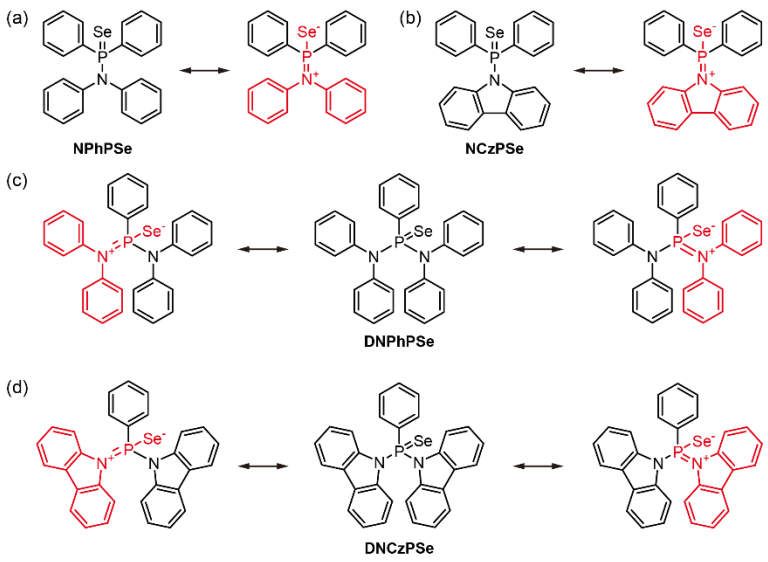

Scheme S2. Main resonance structures of (a) **NPhPSe**, (b) **NCzPSe**, (c) **DNPhPSe** and (d) **DNCzPSe**.

4. Materials and Synthesis

The synthetic route of the N-P=Se resonance molecules was illustrated in **Scheme S3**.

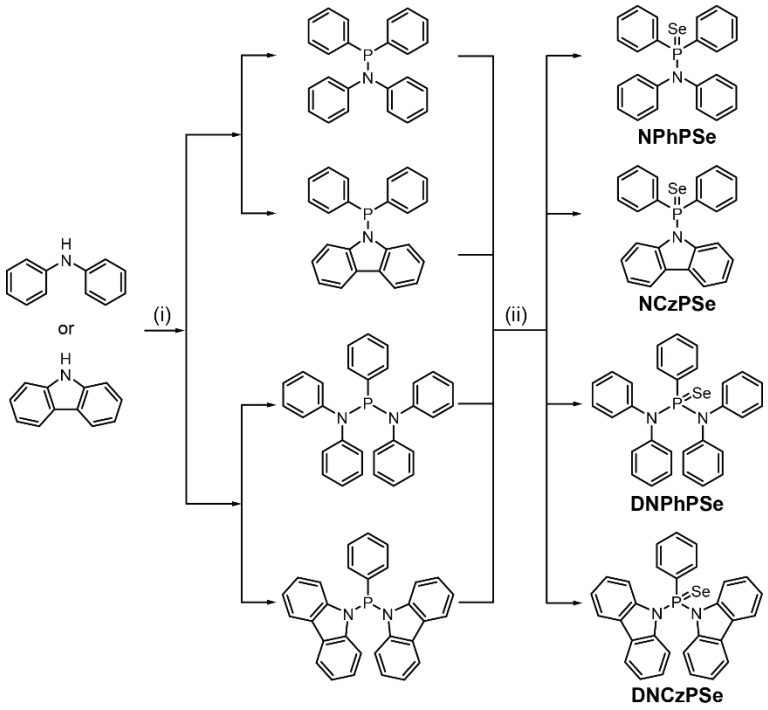

Scheme S3. Synthetic route of the N-P=Se resonance molecules: (i) *n*-BuLi, THF, -78ºC, 1 h followed by Ph_2Cl or $PhCl_2$, -78ºC, overnight; (ii) Selenium, $CHCl_3$, 55ºC, 5 h.

Synthesis of (N,N-diphenyl)diphenylphosphine selenide (NPhPSe): To a freshly distilled THF (50 mL) solution of diphenylamine (2.0 g, 11.8 mmol) at -78°C under nitrogen atmosphere was added dropwise a hexane solution of *n*-butyl lithium (5.7 mL, 14.2 mmol, 2.5 M in hexane). After lithiation at -78°C for 1 h, diphenylphosphine chloride (2.8 mL, 15.4 mmol) was added into the reaction system rapidly. The reaction mixture at -78°C was allowed to warm to room temperature and stirred overnight.[8, 9] Then, the reaction was quenched with water (10 mL) and extracted with dichloromethane (DCM) (3×30 mL). The organic layers were collected and dried with anhydrous Na_2SO_4. The organic solvent was removed under reduced pressure. The residue was dissolved without further purification in chloroform (50 mL) and selenium (1.87 g, 23.64 mmol) was added into for the following selenylation. After the reaction mixture was stirred 5 h at 55°C, water (10 mL) was added to quench the reaction. The mixture was extracted with DCM (3×30 mL) and the collected organic layers were dried with anhydrous Na_2SO_4. The organic solvent was removed under reduced pressure. The resulting crude product was purified by flash column chromatography on silica gel. Yield: 70%, white powder. ^{1}H NMR (DMSO-d_6, 400 MHz) δ(ppm): 8.03 (dd, *J*=20 Hz, 4H), 7.45-7.29 (m, 10H), 7.16 (t, *J*=16 Hz, 4H), 7.03 (d, *J*=16 Hz, 2H). ^{13}C NMR ($CDCl_3$, 100 MHz)

δ(ppm): 144.36, 144.34, 133.22, 133.12, 132.58, 131.60, 131.57, 128.66, 128.13, 128.00, 127.26, 127.21, 124.92. ^{31}P NMR (DMSO-d_6, 162.0 MHz) δ(ppm): 63.62 (^{1}J(^{31}P-^{77}Se)=775.98 Hz). ^{77}Se NMR (DMSO-d_6, 76.3 MHz) δ(ppm): -226.52 (^{1}J(^{31}P-^{77}Se)=774.45 Hz). Anal. calcd for $C_{24}H_{20}NPSe$: C 66.67, H 4.66, N 3.24; found: C 66.79, H 4.66, N 2.87.

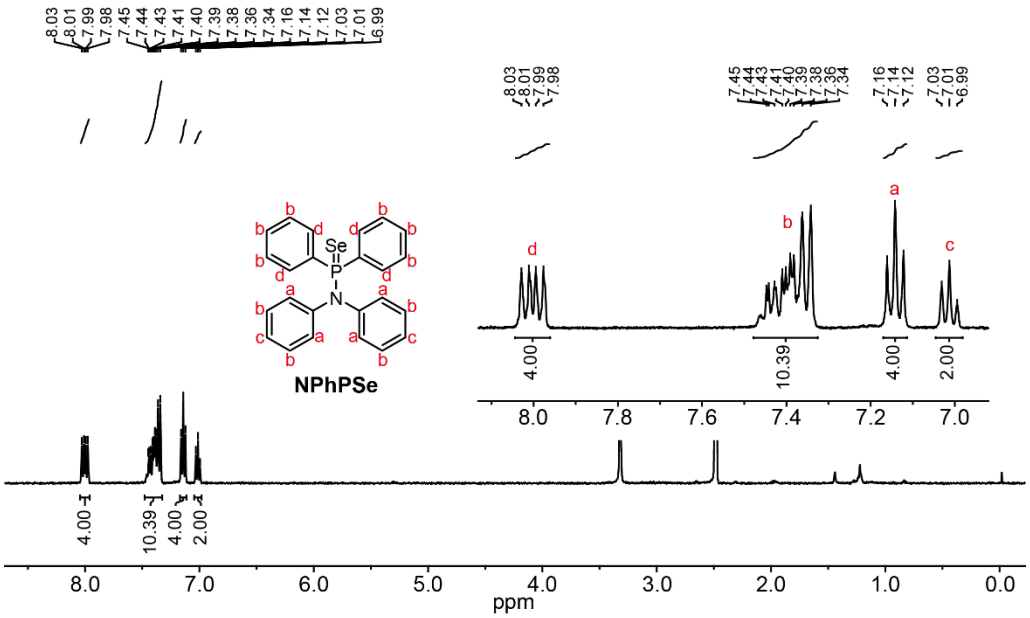

Figure S1. ^{1}H NMR spectrum of **NPhPSe** in DMSO-d_6.

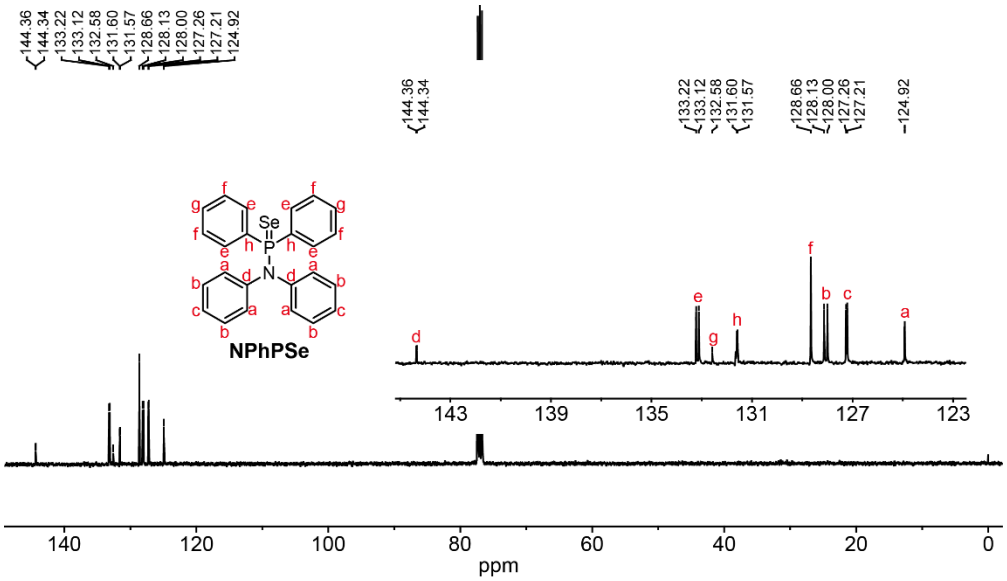

Figure S2. ^{13}C NMR spectrum of **NPhPSe** in $CDCl_3$.

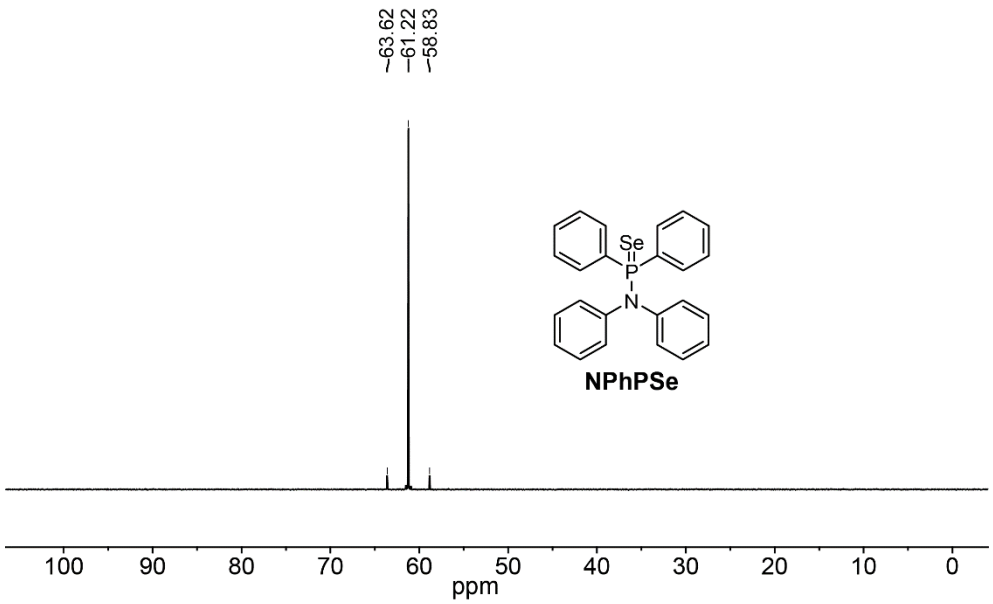

Figure S3. ^{31}P NMR spectrum of **NPhPSe** in DMSO-d_6.

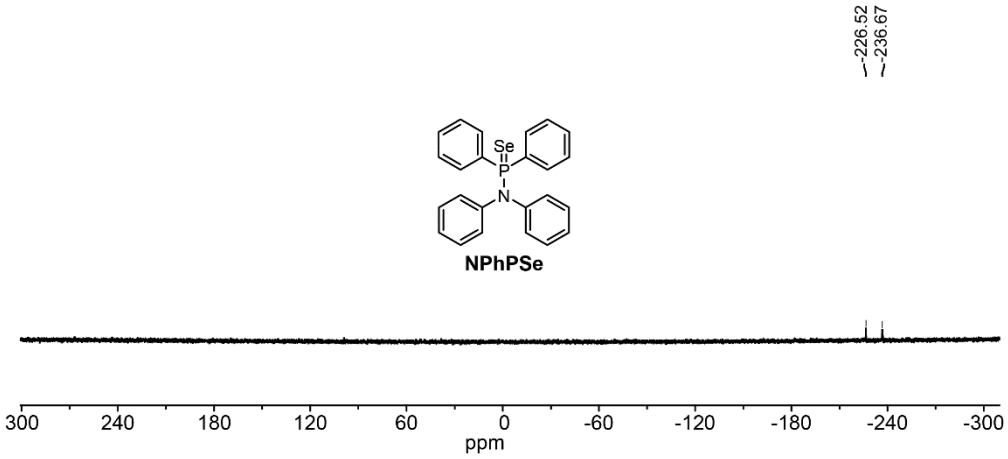

Figure S4. ^{77}Se NMR spectrum of **NPhPSe** in DMSO-d_6.

Synthesis of (9*H*-carbazol-9-yl)diphenylphosphine selenide (NCzPSe): NCzPSe was prepared in an identical synthetic procedure of **NPhPSe** using carbazole (2.0 g, 11.96 mmol), *n*-Butyl lithium (5.7 mL, 14.4 mmol, 2.5 M in hexane), diphenylphosphine chloride (2.8 mL, 15.6 mmol) and Se (1.89 g, 23.92 mmol). Yield: 70%, white powder. ^{1}H NMR (DMSO-d_6, 400 MHz) δ(ppm): 8.20 (d, *J*=8 Hz, 2H), 8.11-8.05 (m, 4H), 7.73-7.70 (m, 2H), 7.66 (td, *J*=20 Hz, 4H), 7.28 (t, *J*=16 Hz, 2H), 7.12-7.08 (m, 2H), 6.47 (d, *J*=8 Hz, 2H). ^{13}C NMR ($CDCl_3$, 100 MHz) δ(ppm): 141.31, 133.05, 132.93, 132.77, 132.74, 132.32, 131.42, 129.08, 128.95, 127.11, 127.06, 125.78, 121.96, 119.92, 115.49, 115.47. ^{31}P NMR (DMSO-d_6, 162.0 MHz) δ(ppm): 56.88 (^1J(^{31}P-^{77}Se)=811.62 Hz). ^{77}Se NMR (DMSO-d_6, 76.3 MHz) δ(ppm): -226.52 (^1J(^{31}P-^{77}Se)=812.60 Hz). Anal. calcd for $C_{24}H_{18}NPSe$: C 66.98, H 4.22, N 3.25; found: C 66.83, H 4.28, N 2.88.

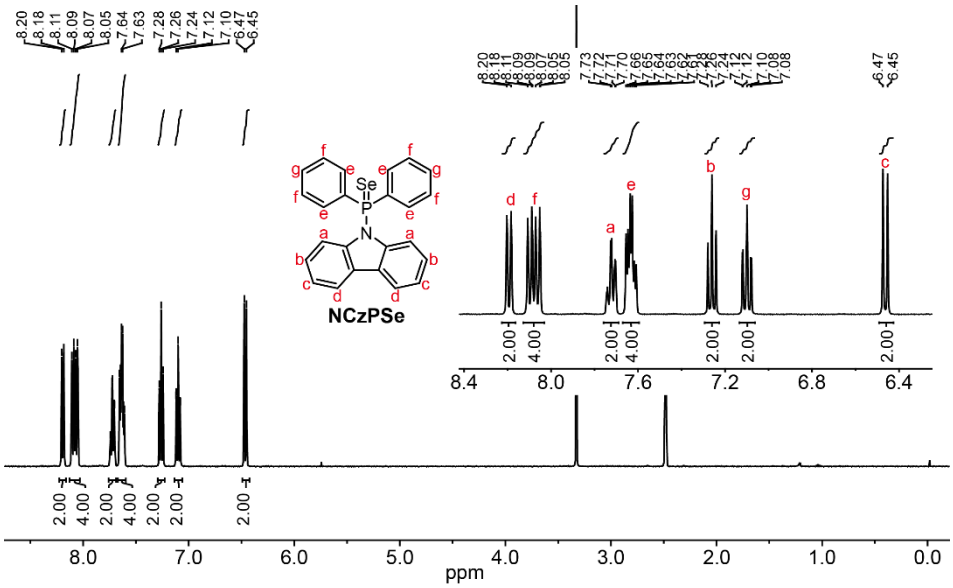

Figure S5. ^{1}H NMR spectrum of **NCzPSe** in DMSO-d_6.

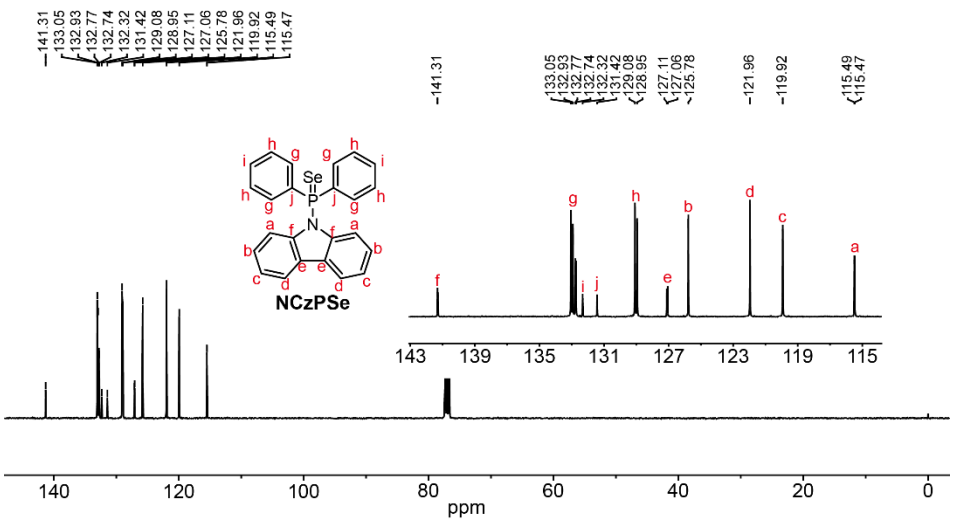

Figure S6. ^{13}C NMR spectrum of **NCzPSe** in $CDCl_3$.

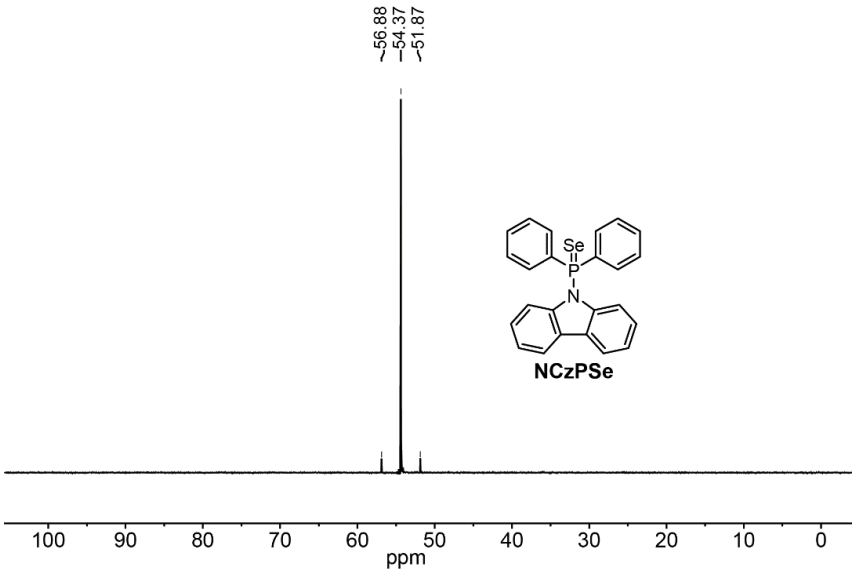

Figure S7. ^{31}P NMR spectrum of **NCzPSe** in DMSO-d_6.

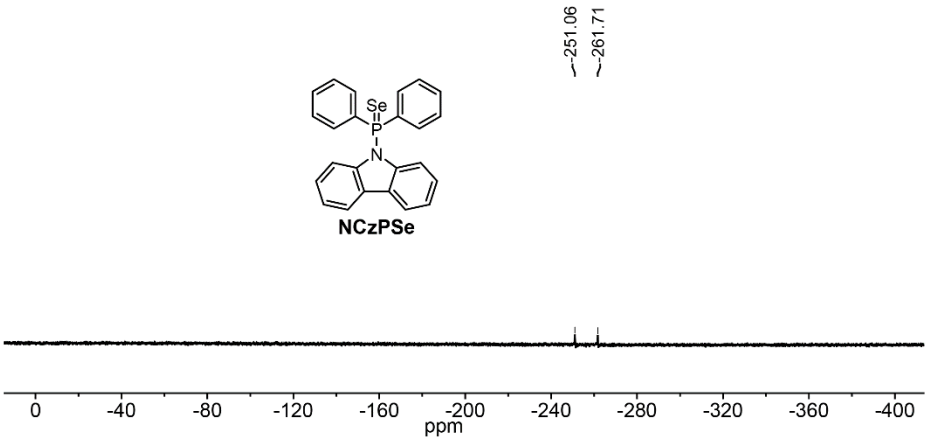

Figure S8. ^{77}Se NMR spectrum of **NCzPSe** in DMSO-d_6.

Synthesis of di(N,N-diphenyl)(phenyl)phosphine selenide (DNPhPSe): DNPhPSe was prepared in an identical synthetic procedure of **NPhPSe** using diphenylamine (2.0 g, 11.82 mmol), *n*-Butyl lithium (5.7 mL, 14.2 mmol, 2.5 M in hexane), and dichlorophenylphosphine (0.8 mL, 5.9 mmol) and Se (1.87 g, 23.64 mmol). Yield: 50%, white powder. ^{1}H NMR (DMSO-d_6, 400 MHz) δ(ppm): 7.70-7.65 (m, 2H), 7.36-7.32 (m, 1H), 7.25-7.20 (m, 18H), 7.15-7.11 (m, 4H). ^{13}C NMR ($CDCl_3$, 100 MHz) δ(ppm): 144.97, 144.93, 134.70, 133.58, 133.47, 131.23, 131.20, 128.81, 128.78, 128.68, 127.28, 127.14, 125.88. ^{31}P NMR (DMSO-d_6, 162.0 MHz) δ(ppm): 68.14 (^1J(^{31}P-^{77}Se)=814.86 Hz). ^{77}Se NMR (DMSO-d_6, 76.3 MHz) δ(ppm): -98.89 (^1J(^{31}P-^{77}Se)=812.60 Hz). Anal. calcd for $C_{30}H_{25}N_2PSe$: C 68.83, H 4.81, N 5.35; found: C 68.61, H 4.79, N 4.87.

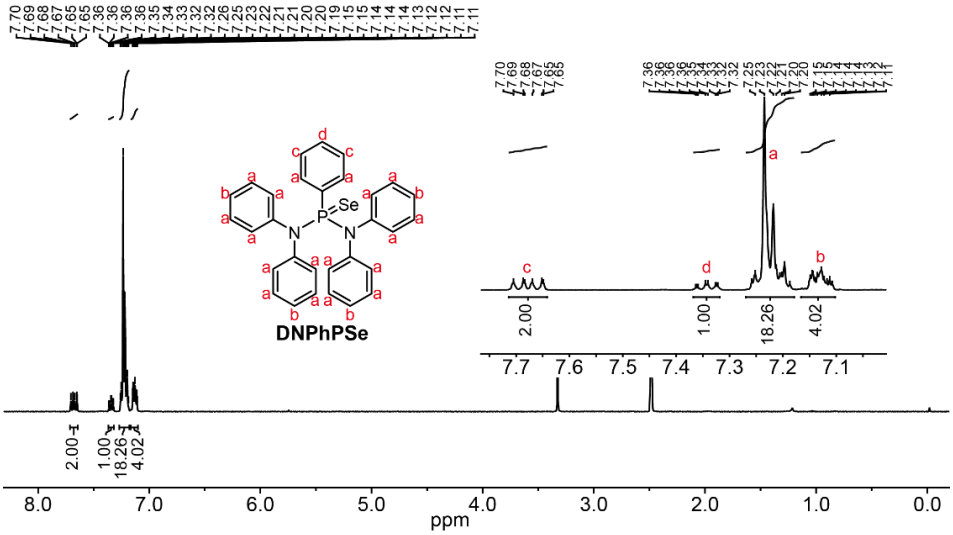

Figure S9. ^{1}H NMR spectrum of **DNPhPSe** in DMSO-d_6.

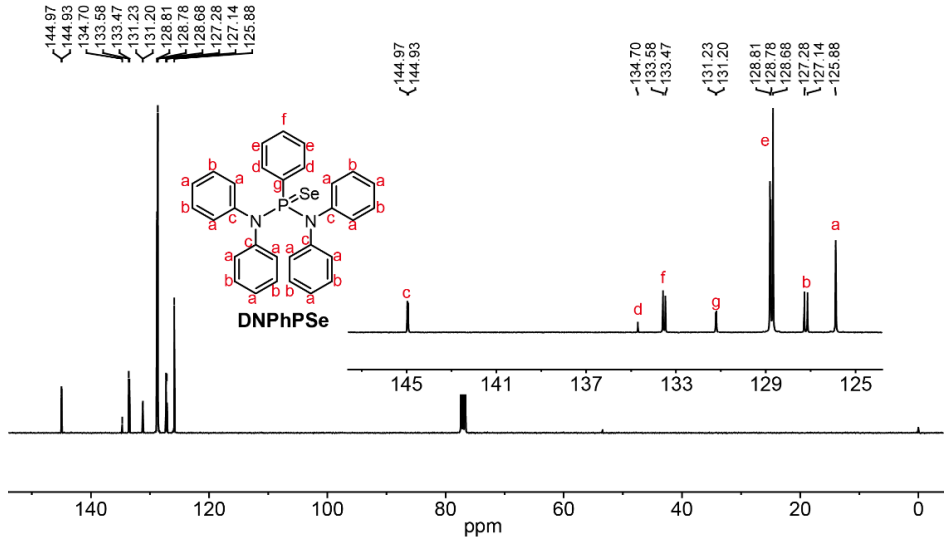

Figure S10. ^{13}C NMR spectrum of **DNPhPSe** in $CDCl_3$.

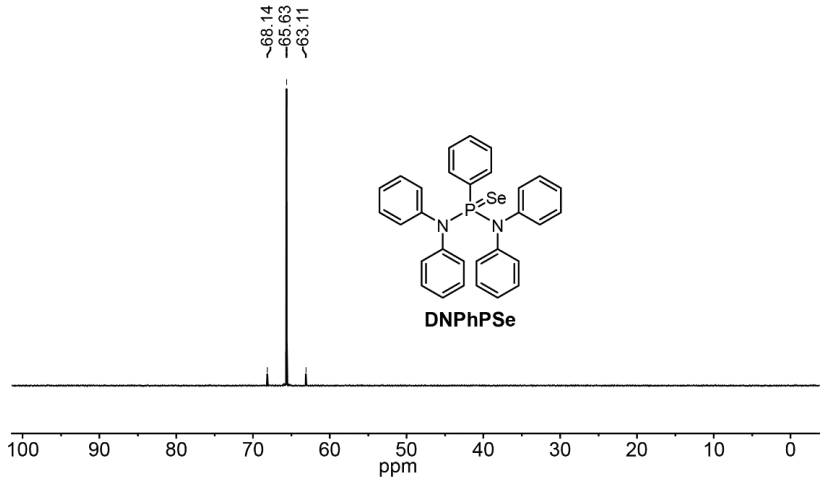

Figure S11. ^{31}P NMR spectrum of **DNPhPSe** in DMSO-d_6.

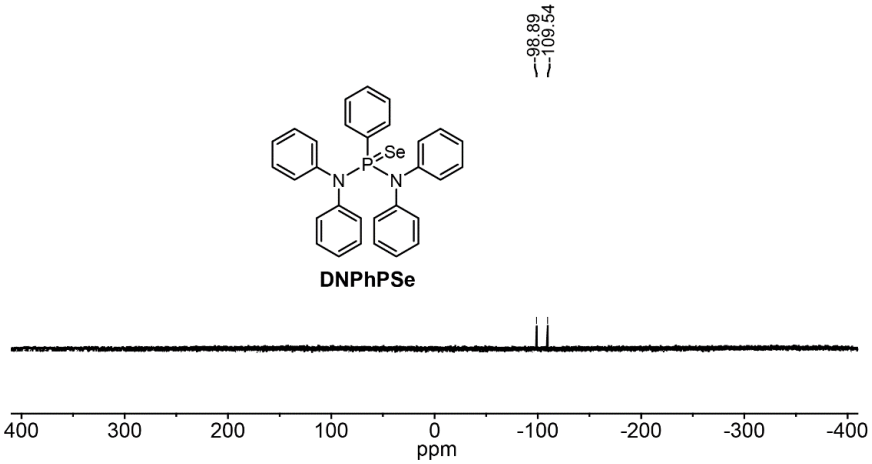

Figure S12. ^{77}Se NMR spectrum of **DNPhPSe** in DMSO-d_6.

Synthesis of di (9*H*-carbazol-9-yl) phenylphosphine selenide (DNCzPSe): DNCzPSe was prepared in an identical synthetic procedure of **NPhPSe** using carbazole (2.0 g, 11.96 mmol), *n*-Butyl lithium (5.7 mL, 14.4 mmol, 2.5 M in hexane), and dichlorophenylphosphine (0.8 mL, 6.0 mmol) and Se (1.89 g, 23.92 mmol). Yield: 70%, white powder. ^{1}H NMR (DMSO-d_6, 400 MHz) δ(ppm): 8.24 (d, *J*=8 Hz, 4H), 8.06-8.00 (m, 2H), 7.90-7.87 (t, *J*=12 Hz, 1H), 7.75 (td, *J*=16 Hz, 2H), 7.32 (t, *J*=16 Hz, 4H), 7.16-7.06 (m, 8H). ^{13}C NMR ($CDCl_3$, 100 MHz) δ(ppm): 140.90, 140.86, 134.26, 134.23, 133.77, 133.63, 133.27, 132.19, 129.54, 129.39, 127.13, 127.07, 126.32, 122.73, 119.94, 115.64. ^{31}P NMR (DMSO-d_6, 162.0 MHz) δ(ppm): 52.42 (^1J(^{31}P-^{77}Se)=810.00 Hz). ^{77}Se NMR (DMSO-d_6, 76.3 MHz) δ(ppm): -100.03 (^1J(^{31}P-^{77}Se)=871.35 Hz). Anal. calcd for $C_{30}H_{21}N_2PSe$: C 69.37, H 4.08, N 5.39; found: C 69.01, H 4.17, N 5.01.

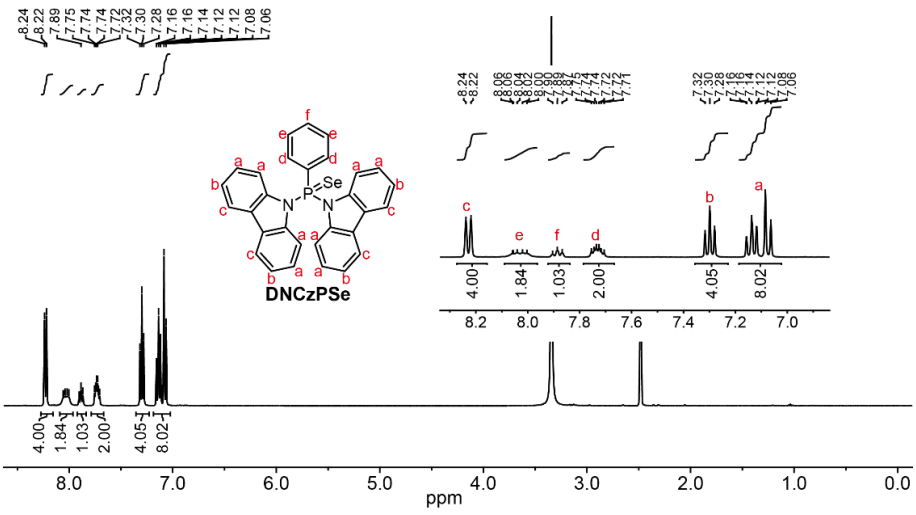

Figure S13. ^{1}H NMR spectrum of **DNCzPSe** in DMSO-d_6.

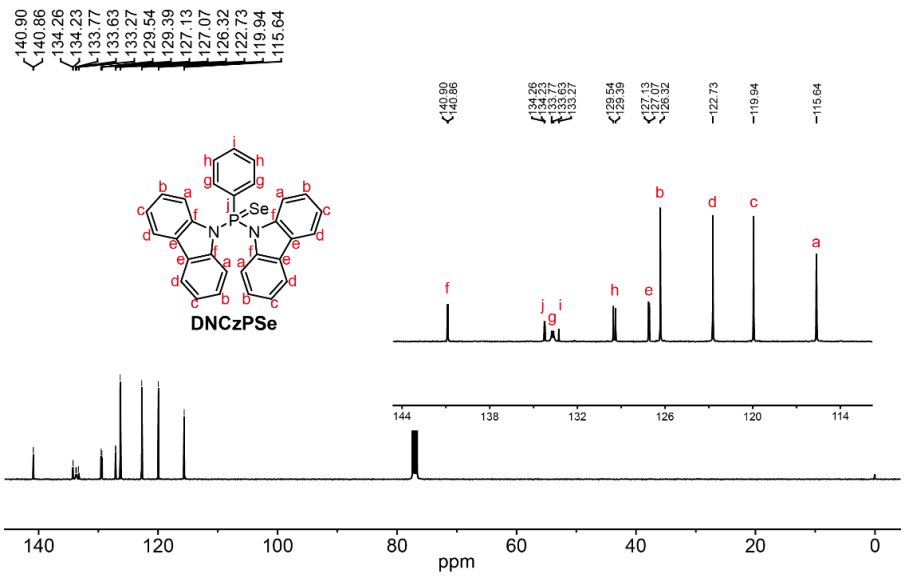

Figure S14. ^{13}C NMR spectrum of **DNCzPSe** in $CDCl_3$.

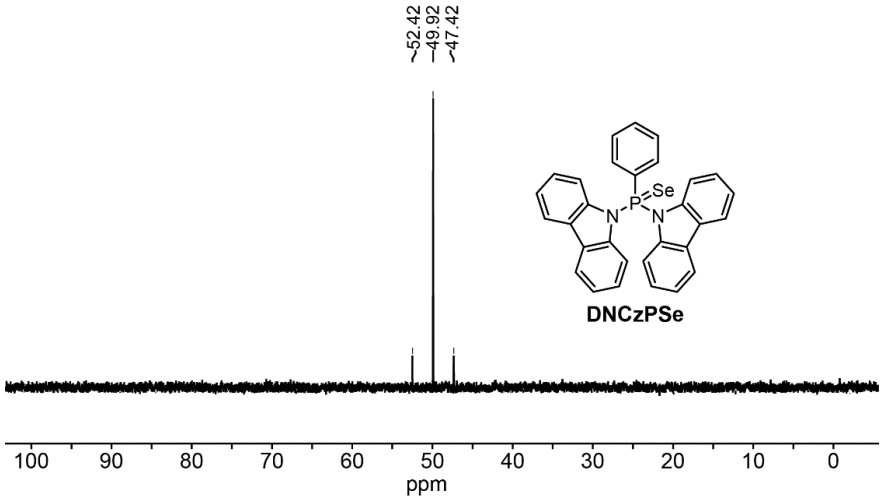

Figure S15. ^{31}P NMR spectrum of **DNCzPSe** in DMSO-d_6.

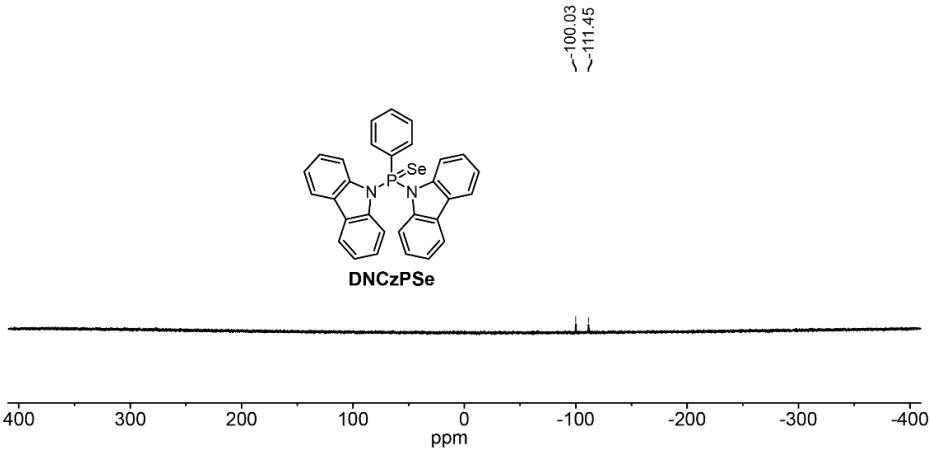

Figure S16. ^{77}Se NMR spectrum of **DNCzPSe** in DMSO-d_6.

5. Single Crystal X-ray Analysis

Single crystals of **NCzPSe**, **DNPhPSe** and **DNCzPSe** were grown by slow evaporation of a combined dichloromethane and ethanol solution at room temperature. Data of single crystal structures were collected on a Bruker SMART APEX (II)-CCD at 296 K. Their crystallographic data were summarized in **Table S1**. The crystallographic information files (CIF) with CCDC deposition numbers of 1813440, 1813443 and 1813444 were also attached.

Table S1. Crystallographic data for **NCzPSe**, **DNPhPSe**, and **DNCzPSe** single crystals

Compound	**NCzPSe**	**DNPhPSe**	**DNCzPSe**
Empirical formula	$C_{24}H_{18}NPSe$	$C_{30}H_{25}N_2PSe$	$C_{30}H_{21}N_2PSe$
Formula weight (g mol^{-1})	430.35	524.09	519.42
Crystal color	colorless	colorless	colorless
Wavelength (Å)	0.71073	0.71073	0.71073
Crystal system	Triclinic	Monoclinic	Triclinic
Space group	P-1	$P2_1/n$	P-1
a (Å)	9.689(3)	11.612(3)	9.5713(14)
b (Å)	9.904(3)	17.433(5)	11.6043(17)
c (Å)	11.312(4)	12.594(3)	12.0406(17)
α (deg)	95.848(7)	90	72.019(3)
β (deg)	101.924(7)	103.247(6)	68.768(3)
γ (deg)	111.026(6)	90	73.861(3)
V ($Å^3$)	972.8(5)	2481.5(11)	1164.7(3)
Z	2	4	2
Density (g cm^{-3})	1.469	1.401	1.481
μ (mm^{-1})	2.02	1.599	1.703
T_{min}, T_{max}	0.794, 0.823	0.831, 0.857	0.822, 0.848
F(000)	436	1072	528
h_{max}, k_{max}, l_{max}	12, 13, 15	18, 27, 19	11, 9, 14
$Theta_{max}$	28.33	33.67	28.25

6. Solubility and Thermal Properties

Solubility tests were made in tetrahydrofuran (THF), toluene, dichloromethane (CH_2Cl_2), and trichloromethane ($CHCl_3$) at room temperature. Thermogravimetric analyses (TGA) were conducted on a DTG-60 Shimadzu thermal analyst system under a heating rate of 10ºC/min and a nitrogen flow rate of 50 cm^3/min. The differential scanning calorimetry (DSC) analyses were performed on a Netzsch DSC-214 instrument under a heating rate of 10ºC/min and a nitrogen flow rate of 20 cm^3/min. The compounds show good thermal property with high decomposition temperature (T_d) and melting temperature (T_m) up to 303 ºC and 290 ºC.

Table S2. Solubility tests of the N-P=Se resonance molecules. (in mg mL^{-1}).

Compound	**NPhPSe**	**NCzPSe**	**DNPhPSe**	**DNCzPSe**
THF	181	74	236	32
Toluene	49	18	100	28
CH_2Cl_2	313	96	343	26
$CHCl_3$	349	114	398	22

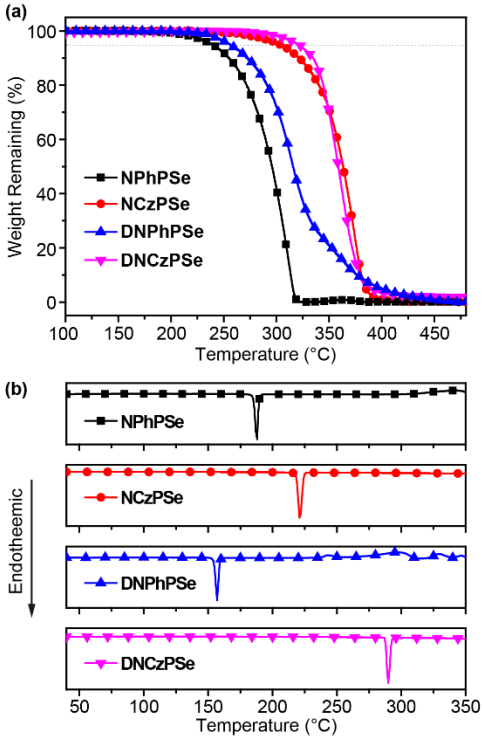

Figure S17. (a) TGA and (b) DSC curves of the N-P=Se resonance molecules.

7. Optical Properties

Ultraviolet/visible (UV/Vis) absorption spectra were recorded on a Lambda 650 S Perkin Elmer UV/VIS spectrophotometer. Fluorescence spectra were measured on an Edinburgh FLS920 fluorescence spectrophotometer with a Xenon lamp. Fluorescence spectra of **NCzPSe** and **DNCzPSe** in tetrahydrofuran (THF) at different concentrations from 20 μM to 100 μM were shown in **Figure S10**. The fluorescence intensity of **NCzPSe** and **DNCzPSe** solution reduces gradually with increasing concentrations (20-100 μM) (**Figures S10a** and **S10b**).[3] The fluorescence spectra of N-P intermediate of **NCzP** before and after selenizing were shown in **Figure S19**. No fluorescence change upon NaClO addition can be observed, indicating that the N-P intermediate is neither a "turn on" nor "turn off" probe; the turn-on detection behavior of the Se-containing resonance molecules towards HClO is closely related to the Se atom. The rate of response was investigated by time dependent fluorescence intensity change (**Figure S19**) by gradually adding batches of NaClO aqueous solution (10 μL, 0.05 μM) into the NCzPSe THF solution (2.0 mL, 1.0 μM). Almost immediate enhance of fluorescent strength were observed, when each batches of NaClO solution (10 μL, 0.05 μM) was added into the probe solution, indicating clearly their rapid response to HClO. The high selectivity of these HClO probes can be confirmed by screening experiments of probes with low concentration of NaClO and high concentration of other different analytes (**Figure 3**).

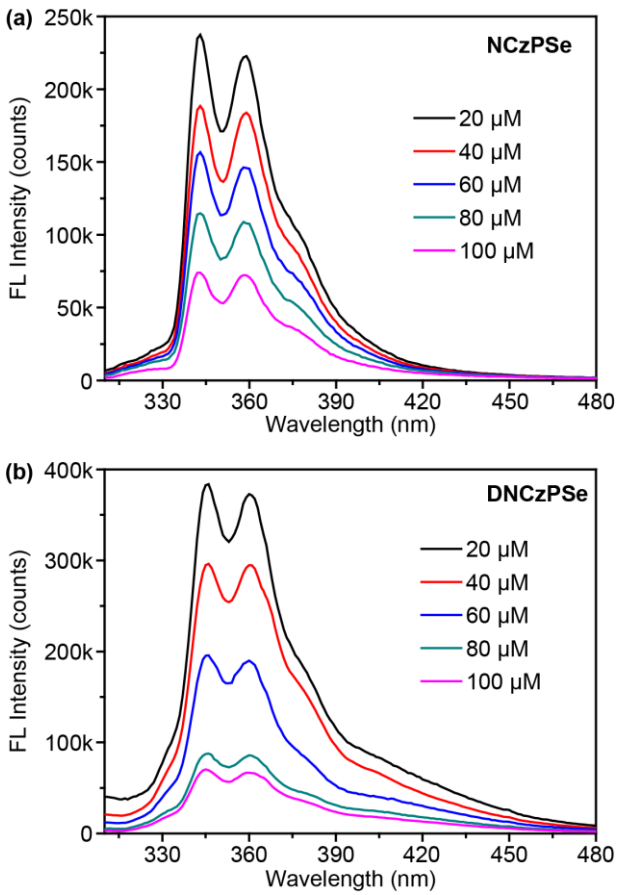

Figure S18. Fluorescence spectra of (a) **NCzPSe** (b) **DNCzPSe** at different concentrations from 20 to 100 μM in PBS buffer (pH=7.4, 20 mM). The excitation wavelength was set to be 295 nm.

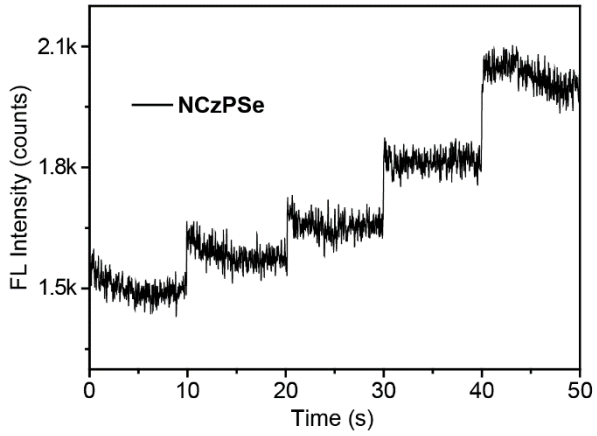

Figure S19. Time dependent fluorescence (345 nm) intensity changes of **NCzPSe** in THF (2.0 mL, 1.0 μM) with gradual addition of batches of NaClO aqueous solution (10 μL, 0.05 μM) on excitation at 295 nm.

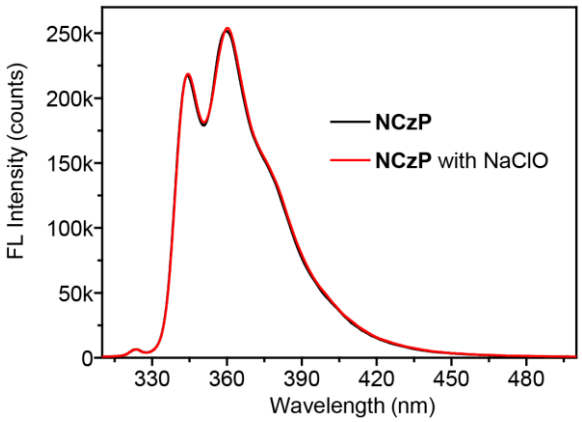

Figure S20. Fluorescence spectra of NCzP in THF (2.0 mL, 1.0 μM) excited at 295 nm with or without sodium hypochlorite (NaClO) aqueous solution (10 μL, 100 μM).

8. HClO Detection Mechanism

We suppose that the reaction mechanism for the detection of HClO is due to the oxidation of Se in the N-P=Se resonance linkage.[5,7,10] As a typical example, the structure change from **NCzPSe** to its oxidized from after reaction with HClO were illustrated in **Scheme S3**. Further, the ^{1}H NMR, ^{13}C NMR, ^{31}P NMR and ^{77}Se NMR spectra of **NCzPSe** and oxidized **NCzPSe** were recorded on a Bruker Ultra Shield Plus 400 MHz instrument with DMSO-d_6 as the solvents. The oxidized **NCzPSe**: ^{1}H NMR (DMSO-d_6, 400 MHz) δ(ppm): 8.03 (d, J=8 Hz, 2H), 7.81 (ddd, J=20 Hz, 4H), 7.46 (d, J=8 Hz, 2H), 7.29-7.24 (m, 8H), 7.02-6.98 (m, 2H). ^{13}C NMR (DMSO-d_6, 100 MHz) δ(ppm): 152.12, 146.45, 145.57, 130.77, 130.67, 129.13, 129.10, 127.56, 127.45, 124.32, 122.14, 119.14, 115.53, 112.42. ^{31}P NMR (DMSO-d_6, 162.0 MHz) δ(ppm): 46.26 (^{1}J(^{31}P-^{77}Se)=644.76). ^{77}Se NMR (DMSO-d_6, 76.3 MHz) δ(ppm): -90.90 (^{1}J(^{31}P-^{77}Se)=645.50).

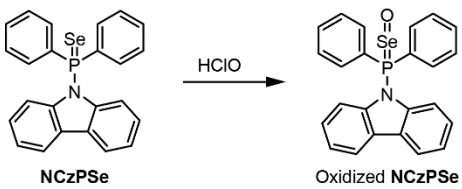

Scheme S4. Proposed mechanism for the detection of HClO.

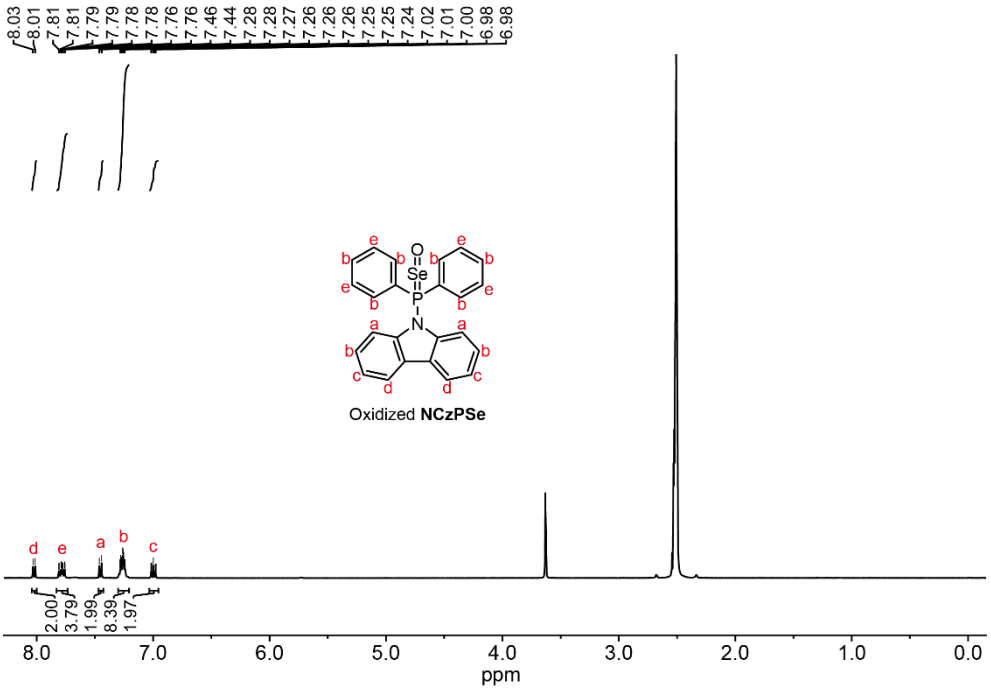

Figure S21. ^{1}H NMR spectrum of the oxidized **NCzPSe** in DMSO-d_6.

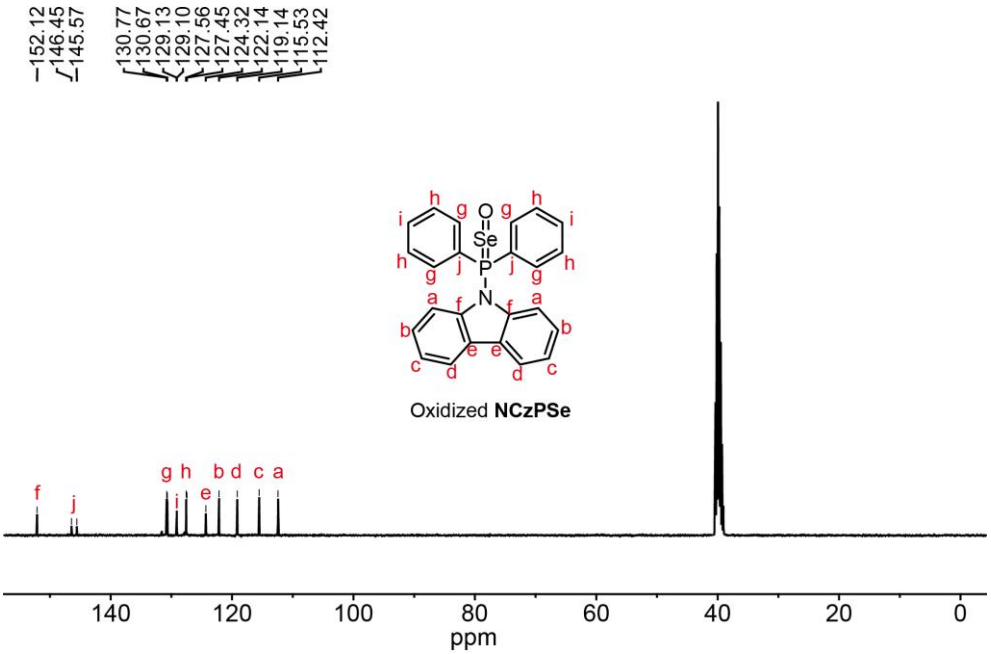

Figure S22. ^{13}C NMR spectrum of the oxidized **NCzPSe** in DMSO-d_6.

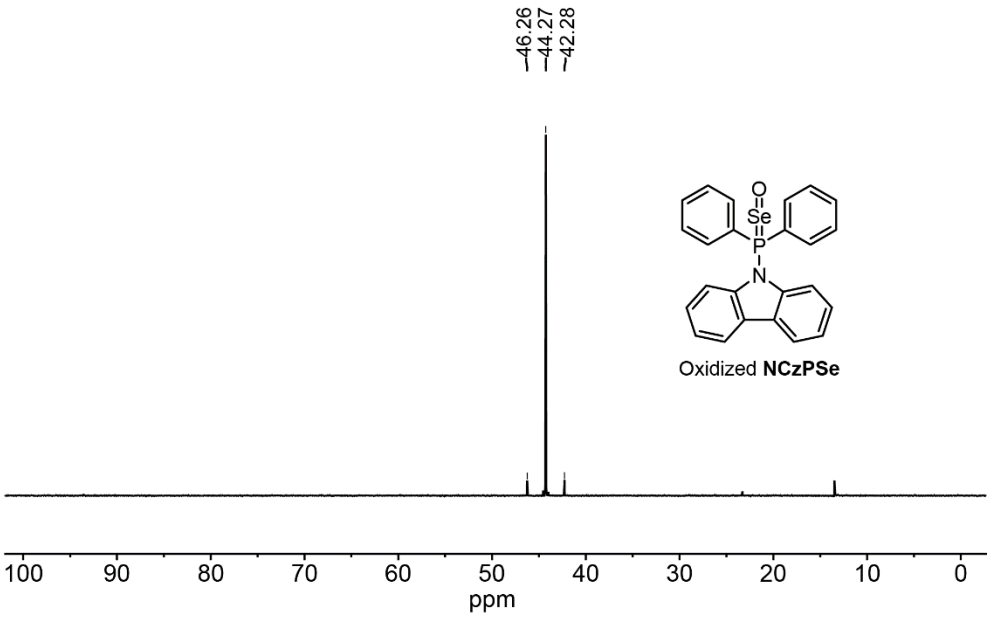

Figure S23. ^{31}P NMR spectrum of the oxidized **NCzPSe** in DMSO-d_6.

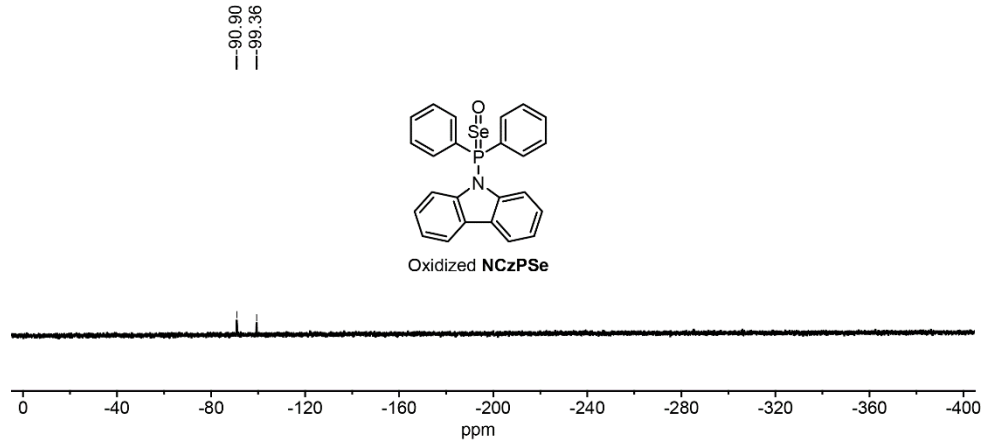

Figure S24. ^{77}Se NMR spectrum of the oxidized **NCzPSe** in DMSO-d_6.

9. Theoretical Calculations

Density functional theoretical (DFT) calculations were performed on Gaussian 09 program. The ground state (S_0) structures of the resonance molecules were optimized using B3LYP with 6-31G(d) basis set.[10] The fuzzy bond order analysis was using Multiwfn.[11, 12] The highest occupied molecular orbital (HOMO), the lowest unoccupied molecular orbital (LUMO) energy levels, and frontier molecular orbitals distributions were predicted by B3LYP/6-31G(d) based on the optimized S_0 geometries using M06-2X/cc-pVTZ, since B3LYP/6-31G(d) is good in predicting the molecular energy levels of organic optoelectronic molecules.[13]

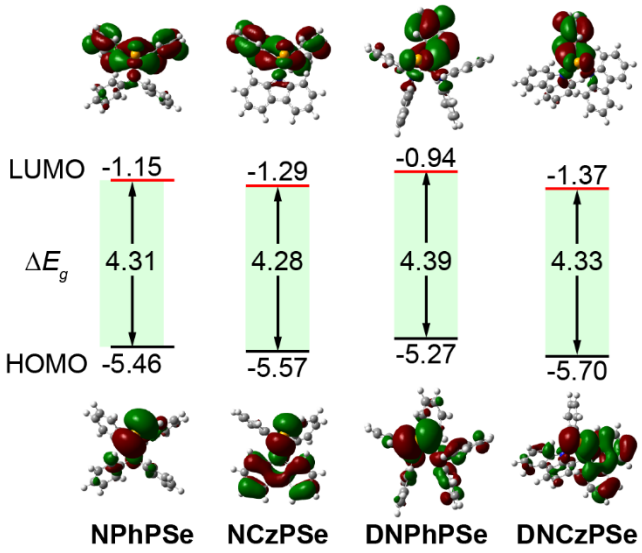

Figure S25. DFT calculated HOMO and LUMO energy levels, and frontier molecular orbitals distributions of the N-P=Se resonance molecules.

Figure S26. Frontier molecular orbital distributions of **NCzPSe** and oxidized **NCzPSe**.

	NCzPSe	Oxidized **NCzPSe**
LUMO+4	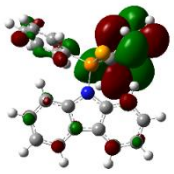 -0.39 eV	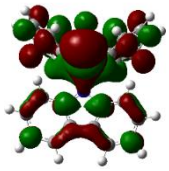 -0.33 eV
LUMO+3	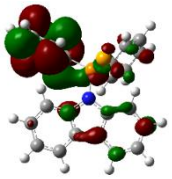 -0.44 eV	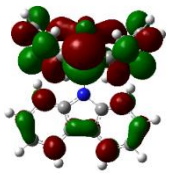 -0.66 eV
LUMO+2	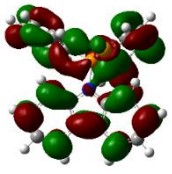 -0.65 eV	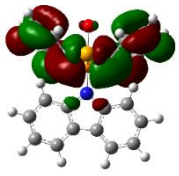 -0.68 eV

LUMO+1	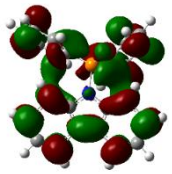 -0.83 eV	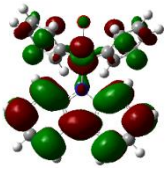 -1.06 eV
LUMO	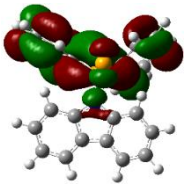 -1.29 eV	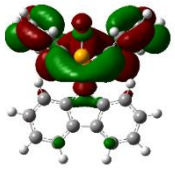 -1.49 eV
HOMO	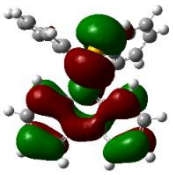 -5.57 eV	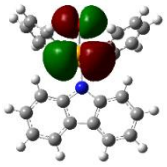 -4.33 eV
HOMO-1	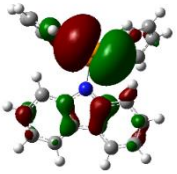 -5.71 eV	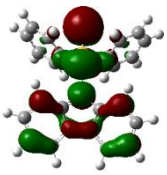 -5.55 eV
HOMO-2	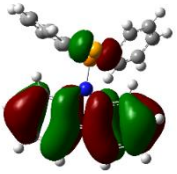 -5.80 eV	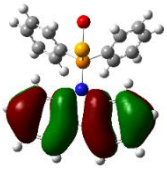 -6.09 eV
HOMO-3	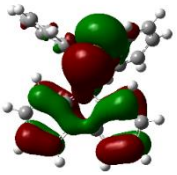 -5.94 eV	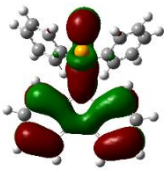 -6.30 eV

Table S3. Absorption band with the largest oscillator strength (*f*) of **NCzPSe** and its oxidized form.

Compound	*f*	Transition configuration
NCzPSe	0.0304	HOMO-3→LUMO+1 (8.06%) HOMO-2→LUMO+1 (68.52%) HOMO-2→LUMO+2 (7.43%) HOMO-1→LUMO+2 (5.55%) HOMO→LUMO+4 (4.79%)
Oxidized **NCzPSe**	0.0260	HOMO-1→LUMO+2 (83.92%) HOMO-1→LUMO+3 (9.73%)

Table S4. Fuzzy bond order analysis of the N-P=Se resonance molecules.

Compound	Bond order		
	N-P	P=Se	C-P
NPhPSe	1.27	1.77	1.03/1.02
NCzPSe	1.22	1.78	1.03/1.04
DNPhPSe	1.26/1.25	1.68	1.01
DNCzPSe	1.22/1.23	1.79	1.04
NPhPSeO	1.29	1.33	1.05/1.06
NCzPSeO	1.27	1.33	1.04/1.05
DNPhPSeO	1.30/1.30	1.21	1.07
DNCzPSeO	1.26/1.23	1.24	1.04

10. Time-Resolved Transient Fluorescence Decay

Time-resolved transient fluorescence decay curves were recorded on an Edinburgh FLS920 fluorescence spectrophotometer with 280 nm laser. Time-resolved transient fluorescence decay curve of **NCzPSe** shows shorter fluorescent lifetime (3.05 ns) than its oxidized form (4.79 ns), confirming the reduced quenching effects in oxidized **NCzPSe** (**Figures S15a** and **S15b**).

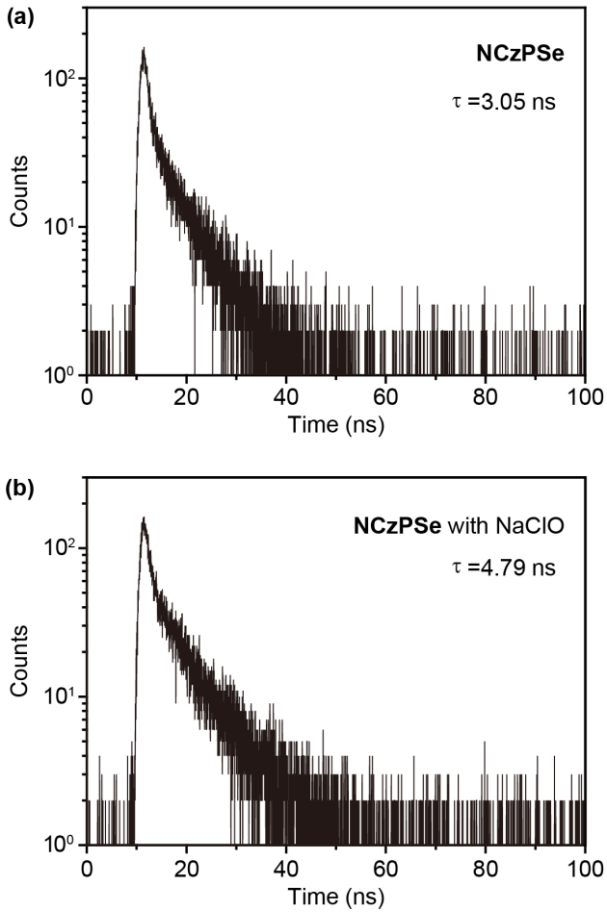

Figure S27. Transient fluorescence (345 nm) decay curves of **NCzPSe** before (a) and after (b) NaClO treatment under the excitation of 280 nm.

References:

1. B. Wang, P. Li, F. Yu, P. Song, X. Sun, S. Yang, Z. Lou, and K. Han, *Chem. Commun*, 2013, **49**, 1014-1016.

2. G. Li, D. Zhu, Q. Liu, L. Xue, and H. Jiang, *Org. Lett*, 2013, **15**, 2002-2005.

3. G. Cheng, J. Fan, W. Sun, J. Cao, C. Hu and X. Peng, *Chem. Commun*, 2014, **50**, 1018-1020.

4. S. T. Manjare, J. Kim, Y. Lee and D. G. Churchill, *Org. Lett*, 2014, **16**, 520-523.

5. Z. Qu, J. Ding, M. Zhao and P. Li, *J. Photoch. Photobio. A*, 2015, **299**, 1-8.

6. W. Zhang, W. Liu, P. Li, J. Kang, J. Wang, H. Wang, and B. Tang, *Chem. Commun*, 2015, **51**, 10150-10153.

7. S. Milay, M. Choi, Y. Jang, Y. Kim, S. Jon, and D. Cherchill, *Chem. Eur. J*, 2016, **22**, 9642-9648.

8. Y. Tao, J. Xiao, C. Zheng, Z. Zhang, M. Yan, R. Chen, X. Zhou, H. Li, Z. An, Z. Wang, H. Xu and W. Huang, *Angew. Chem. Int. Edit*, 2013, **52**, 10491-10495.

9. Y. Tao, L. Xu, Z. Zhang, R. Chen, H. Li, H. Xu, C. Zheng and W. Huang, *J. Am. Chem. Soc*, 2016, **138**, 9655-9662.

10. G. W. T. M. J. Frisch, H. B. Schlegel, G. E. Scuseria, M. A. Robb, J. R. Cheeseman, G. Scalmani, V. Barone, G. A. Petersson, H. Nakatsuji, X. Li, M. Caricato, A. Marenich, J. Bloino, B. G. Janesko, R. Gomperts, B. Mennucci, H. P. Hratchian, J. V. Ortiz, A. F. Izmaylov, J. L. Sonnenberg, D. Williams-Young, F. Ding, F. Lipparini, F. Egidi, J. Goings, B. Peng, A. Petrone, T. Henderson,

D. Ranasinghe, V. G. Zakrzewski, J. Gao, N. Rega, G. Zheng, W. Liang, M. Hada, M. Ehara, K. Toyota, R. Fukuda, J. Hasegawa, M. Ishida, T. Nakajima, Y. Honda, O. Kitao, H. Nakai, T. Vreven, K. Throssell, J. A. Montgomery, Jr., J. E. Peralta, F. Ogliaro, M. Bearpark, J. J. Heyd, E. Brothers, K. N. Kudin, V. N. Staroverov, T. Keith, R. Kobayashi, J. Normand, K. Raghavachari, A. Rendell, J. C. Burant, S. S. Iyengar, J. Tomasi, M. Cossi, J. M. Millam, M. Klene, C. Adamo, R. Cammi, J. W. Ochterski, R. L. Martin, K. Morokuma, O. Farkas, J. B. Foresman, and D. J. Fox, *Journal*, 2016, Revision D.01.

11. T. Lu and F. Chen, *J. Comput. Chem*, 2012, **33**, 580-592.

12. F. Shojaie, *Comput. Theor. Chem*, 2017, **1114**, 55-64.

13. S. Wang, X. Yan, Z. Cheng, H. Zhang, Y. Liu and Y. Wang, *Angew. Chem. Int. Edit*, 2015, **54**, 13068-13072.